Assessing Function and Identifying Modifiers of Protein Isoaspartyl Methyltransferase in Schizosaccharomyces pombe

Author: Kristen Benakis

Assessing Function and Identifying Modifiers of Protein Isoaspartyl Methyltransferase in *Schizosaccharomyces pombe*

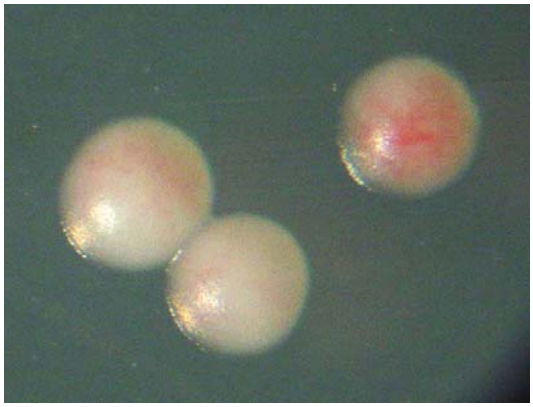

Kristen Benakis

Advisor: Dr. Clare O'Connor

Biology Department

April 30, 2004

Table of Contents

Abstract

Protein isoaspartyl methyltransferase (PIMT), an ancient enzyme with putative homologs in virtually all eukaryotes studied to date, is a protein repair enzyme that initiates restoration of age-damaged isoaspartyl residues back into normal amino acids. I studied the functional importance of PIMT in *Schizosaccharomyces pombe*, whose PIMT-encoding homolog is designated *pcm2*. Past studies of PIMT in other organisms had suggested that Pcm2p function could be important for viability under stress conditions. In the first part of the project, I compared the viability of a yeast strain lacking *pcm2* (*Δpcm2*) under a variety of stress conditions, including stationary phase, heat shock, high-salt, high-sugar, high-pH, and high temperature. Based on studies of PIMT in other organisms, I expected to see reduced viability of the knockout strain during stress conditions, but no difference in cell growth or viability was observed. I also attempted to use Real-Time PCR to compare *pcm2* transcription in yeast under the same stress conditions. I have not yet collected any usable data from the Real-Time PCR runs, but it has been previously shown that *pcm2* transcription increases during stationary phase, heat shock, and osmotic shock. This increase in *pcm2* transcription during stress with no phenotype associated with loss of *pcm2* under stress conditions leads to the hypothesis that there may be a second gene whose product can compensate for loss of PIMT function. To locate and identify this gene, a synthetic lethal screen is being utilized. Currently, five potential synthetic lethal mutants have been isolated.

Chapter 1: Introduction

As proteins age, they undergo many different kinds of spontaneous modifications. These modifications can have various effects. Some might change the shape of the protein; others might compromise the protein's function. One spontaneous modification is the generation of an L-isoaspartate from an L-aspartate or an L-asparagine (see Figure 1). This change is initiated by the nucleophilic attack of the adjacent downstream peptide bond nitrogen onto the side chain carbonyl carbon of an aspartate or asparagine. This produces a succinimide ring with two equivalent peptide bonds, which spontaneously hydrolyzes at one of the two bonds to produce either L-aspartate or L-isoaspartate (Geiger and Clarke 1987). The appearance of an isoaspartyl group introduces an extra carbon into the protein backbone, producing a kink in the protein structure that can interfere with normal folding and function. These damaged amino acids do not accumulate in cells, however, because cells have an isoaspartyl repair mechanism in place. Protein isoaspartyl methyltransferase (PIMT), the focus of my project, is an enzyme that uses S-adenosyl-L-methionine (SAM) as the methyl donor to methylate the carboxyl group of the isoaspartyl residue (Johnson et al 1987). The resulting L-isoaspartyl methyl ester spontaneously demethylates to reform the succinimide ring, which again hydrolyzes at either peptide bond to give L-aspartate or L-isoaspartate (Johnson et al 1987; McFadden and Clarke 1987). The cycle of methylation and demethylation continues until all the L-isoaspartate has been converted into L-aspartate. The net result is the repair of the polypeptide backbone and the conversion of all isoaspartyl residues into aspartyl residues (Johnson et al 1987; Brennan et al 1994). The conversion of L-isoaspartate to L-aspartate allows the protein to regain much of the function that it had lost when the L-isoaspartate first appeared. This gain of function may not be complete if

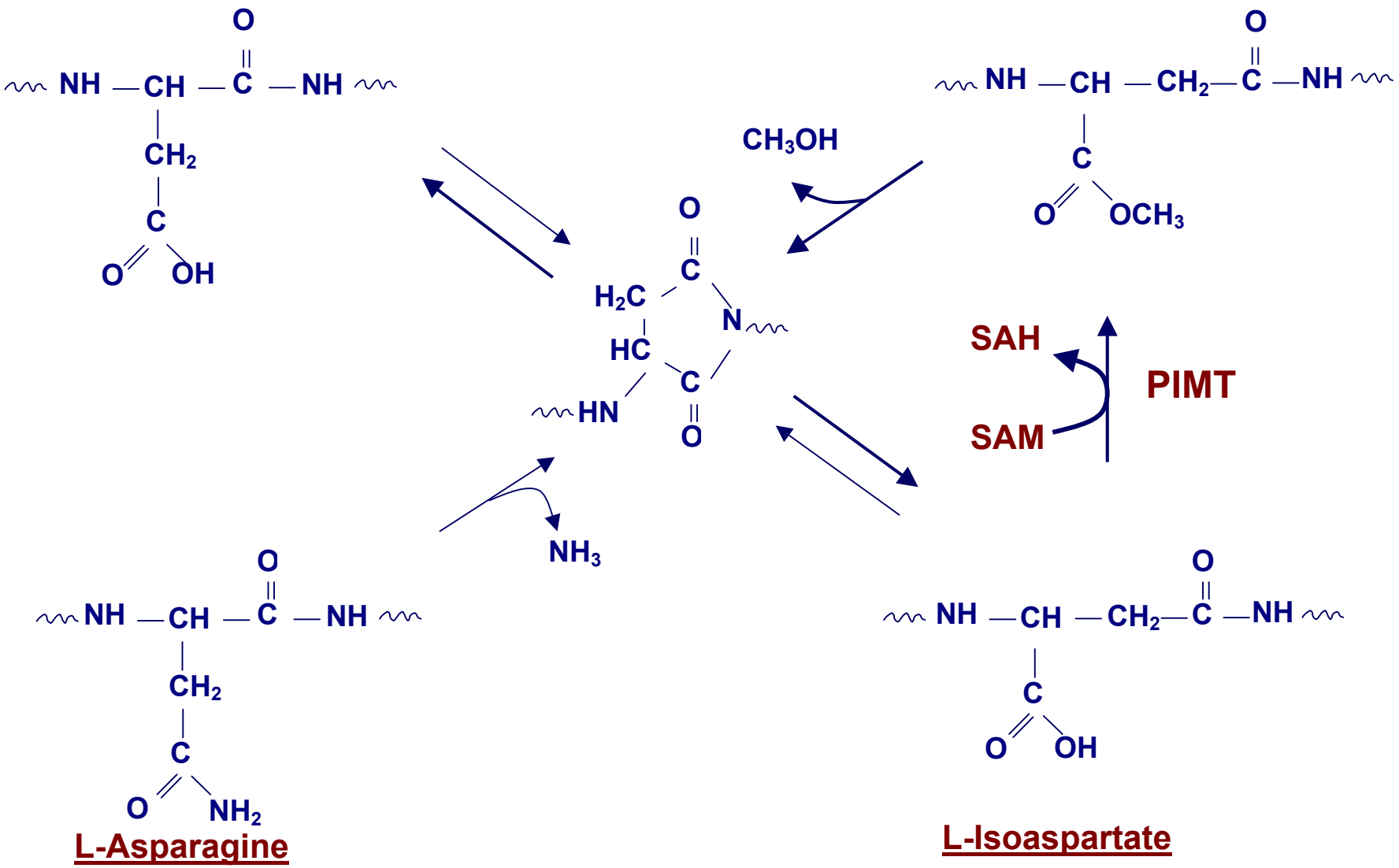

Figure 1

PIMT-mediated protein repair. As proteins age, isoaspartyl residues are spontaneously generated from asparaginyl and aspartyl residues. Protein isoaspartyl methyltransferase (PIMT) initiates repair of this modification by catalyzing the methylation of isoaspartyl residues. The resulting isoaspartyl methyl ester spontaneously demethylates, and can then hydrolyze into an isoaspartyl or an aspartyl residue. The cycle of methylation and demethylation continues until all isoaspartate has been converted to aspartate.

the original damaged amino acid was asparagine, perhaps because any L-isoaspartate generated from L-asparagine becomes L-aspartate in this mechanism, changing the original sequence of the protein.

PIMT enzymatic activity has been demonstrated in a wide variety of organisms, including bacteria, mollusks, fungi, plants, and vertebrates (Johnson et al 1991). In addition, genome-wide screens for sequences capable of encoding PIMT homologs have identified putative PIMT genes in many other species. Potential PIMT-encoding genes have now been found in all eukaryotes studied, except the budding yeast *S. cerevisiae*. Future studies of the enzymatic activities of proteins encoded by these genes may show that they do, in fact, code for PIMT.

In more recent years, gene sequencing and various genome projects have allowed interspecies comparison of different PIMTs. Three highly conserved sequence motifs have been identified throughout SAM-dependent methyltransferases, which include PIMT as well as methyltransferases with a wide range of different substrate specificities (Kagan and Clarke 1994). Because the common feature of these enzymes is their dependence on the cofactor SAM, it is hypothesized that the three conserved motifs are necessary for SAM binding (Kagan and Clarke 1994).

Recently, these predictions have been confirmed by crystal structures of PIMTs from *T. maritima*, *P. furiosus*, *D. melanogaster*, and humans (Skinner et al 2000; Griffith et al 2001; Bennett et al 2003; Ryttersgaard et al 2002; Smith et al 2002). In addition to the SAM binding motifs, the crystal structures have revealed other conserved regions important for binding peptide substrates (Martin and McMillan 2002).

PIMT's strong conservation throughout animal evolution suggests its importance for the viability of organisms, presumably as part of the cellular machinery that deals with protein damage. Experiments with various model organisms have been performed to test this hypothesis. In one such study, an *E. coli* PIMT-deficient mutant was created by homologous recombination. These mutant cells survive normally during both log phase and stationary phase. Their viability is reduced in stationary phase, however, when they are exposed to methanol, paraquat (an oxidative stressor), high salt concentration, or repeated high temperature (Visick et al 1998). This enhanced susceptibility to stresses shows the importance of PIMT during highly stressful conditions.

In a similar study, a *C. elegans* PIMT-deficient mutant was constructed by transposon excision. Once again, these mutants grow and develop normally when compared to controls. However, when mutant worms enter the dauer stage in response to crowding or insufficient food supply, the mutants have a decreased survival rate and decreased fitness compared to control animals (Kagan et al 1997). As with *E. coli*, these results show the importance of PIMT during stress conditions.

A more dramatic effect of PIMT deficiency was observed in mice. PIMT-deficient animals were constructed by targeted disruption of the PIMT in embryonic stem cells, which were then used to produce transgenic animals. The PIMT-deficient mouse exhibits a smaller size, a larger brain, and the appearance of juvenile epilepsy, leading to an early death from seizures (Kim et al 1997; Yamamoto et al 1998). PIMT deficiency also leads to an increased accumulation of isoaspartyl proteins in various tissues, including the brain; it is hypothesized that this accumulation of damaged proteins may lead to the fatal epilepsy (Kim et al 1997). Unfortunately, since these mice die so early, they are not useful for studying the relationship

between PIMT activity and lifespan. These deficits are partially rescued by a transgene that allows PIMT transcription specifically in neural tissue, under the control of a neuron-specific enolase promoter. In rescued mice, the lifespan of the mouse increases to a level intermediate to those of the deficient mouse and the normal mouse, and the size of the rescued mouse is the same as the size of the normal mouse (Lowenson et al 2001). In nonneural tissues of these transgenic PIMT-deficient mice, levels of isoaspartyl proteins were also 5-fold higher than in control animals, yet no apparent defects were found in these tissues, which included the heart, testes, and erythrocytes (Lowenson et al 2001). Thus, damage associated with PIMT loss may be restricted to the brain in mammals.

The effects of PIMT overexpression have been studied in the fruitfly *Drosophila melanogaster*. The lifespan of flies ubiquitously overexpressing PIMT at 3-7 times the normal level increased 32-39 % relative to controls. Lifespan extension was observed when the flies were reared at 29 ˚C but not when the flies were reared at the normal 25 ˚C (Chavous et al 2001). These PIMT overexpressing flies also showed increased locomotor activity relative to controls, throughout the lifespan (Chavous et al 2001). These results once again suggest that PIMT is not necessary for survival at normal conditions, but becomes more important under stress conditions. At the higher temperatures where PIMT extends lifespan, proteins would be more conformationally flexible and susceptible to isoaspartate formation.

The subtle effects observed in most PIMT deletions suggest that other activities may compensate for loss of PIMT function in cells. In this study, I use the fission yeast *S. pombe*, which represents a simple tractable model for studying genetic interactions, to study PIMT function and identify other activities which might substitute for PIMT function. The *S. pombe* homolog of PIMT, Pcm2p, has been shown to be biochemically similar to other PIMTs. Kinetic

data obtained from Pcm2p methylation of ovalbumin (an isoaspartyl-containing substrate) has shown that Pcm2p acts in the same way as other PIMTs (Plodkowski, unpublished data).

Recent genome-wide studies of transcription suggest several situations where Pcm2p function may be especially important. One microarray study characterized the transcriptional regulation of *S. pombe* genes during meiosis and sporulation, which happen under conditions of nutritional stress. This study found *pcm2* transcription to increase over 20-fold following the meiotic divisions and as the yeast began sporulation (Mata et al 2002). A second study used microarrays to characterize transcriptional responses to various other stresses. This study showed that *pcm2* transcription increases over 5-fold in 60 minutes after heat shock to 39 ˚C (Chen et al 2003). These results suggest that, just as in other organisms where PIMT seems to be important under stress conditions, Pcm2p may be important for *S. pombe* survival under stress. Northern blot experiments in our lab further support this idea by demonstrating a large increase in *pcm2* transcription during stationary phase. Moreover, it was shown that *pcm2* transcription increases even more when the stress of stationary phase is combined with the stresses of heat shock to 37˚C or osmotic shock (Northern, unpublished data).

A *pcm2* deficient yeast strain (APP1) has been created by homologous recombination in which a ura^+ gene replaced the endogenous *pcm2* gene (Plodkowski, unpublished data). This *Δpcm2* strain is viable and does not show any difference in growth during log phase, or under various stress conditions including low or high pH, various high temperatures, or high salt conditions (Northern, unpublished data). The increased transcription of *pcm2* during stress conditions with no decreased viability for yeast lacking Pcm2p during those same conditions leads us to hypothesize that a second gene may be compensating for the loss of Pcm2p function.

To find this gene, I am performing a synthetic lethal screen. The strain for this screen, LNP35t, has been constructed previously (Northern, unpublished data). LNP35t was originally *pcm2*-deficient but contains a plasmid carrying the *pcm2* gene. In the synthetic lethal screen, LNP35t is treated with a mutagen and cells are screened to find a mutant which became dependent on *pcm2* as a consequence of losing the other gene that normally compensates for loss of *pcm2*. If this is the only redundant gene, the double mutant would then be dependent on the *pcm2*-containing plasmid for survival, so the cells are screened for those that do not lose the plasmid. My goal is to identify any compensatory genes by mutagenesis and screening, and eventually characterize them.

In addition, I have investigated two other questions: how does the transcription of *pcm2* vary under different stress conditions?; are there phenotypic effects of loss of *pcm2*? For the first, I compare wild-type transcription of *pcm2* during regular log phase growth and under the following stress conditions: stationary phase growth, long-term heat shock, short-term heat shock, high-sugar, high-salt, high pH. I use Real-Time RT-PCR to determine relative levels of *pcm2* for each condition. For the second question, I study the *Δpcm2* strain, APP1, further to identify any effects of *pcm2*-deficiency. Namely, I compare growth of APP1 to that of wild-type yeast during long-term stationary phase culture at normal and elevated temperatures. Also, I compare the growth of APP1 to that of wild-type yeast during the following stress conditions: high-sugar, high-salt, high pH, and each of these combined with elevated temperature.

Chapter 2: Materials and Methods

Materials:

Reagent-grade chemicals and glass beads (425-600 microns) were purchased from Sigma Chemical Company (St. Louis, MO) unless otherwise stated. Granulated agar for solid media, glass beads (4 mm), and culture plates were purchased from Fisher (Pittsburg, PA). Conical tubes were purchased from Becton Dickinson (Franklin Lakes, NJ). SeaKem GTG agarose for nucleic acid gels was purchased from BioWhittaker Molecular Applications (Rockland, ME). Yeast extract, casamino acids, and malt extract were purchased from Difco (Detroit, MI). Tris-HCl was purchased from Polyscience, Inc. (Warrington, PA). Positively charged nylon membranes were purchased from Roche (Indianapolis, IN). Hyblot 3A gel paper was purchased from Denville Scientific (South Plain, NJ). The DECAprime II kit and DNA-*free*™ Dnase treatment and removal kit were purchased from Ambion Corporation (Austin, TX). Micro-columns were purchased from Amersham Biosciences (Piscataway, NJ). Film was purchased from Eastman Kodak Company (Rochester, NY). Cronex Lightning Plus intensifying screens were purchased from DuPont Corporation (Wilmington, DE). Electrophoresis equipment and reagents, the iScript cDNA synthesis kit, the iQ SYBR Green Supermix for Real-Time PCR, and 96-well PCR plates were purchased from Bio-Rad (Hercules, CA). [α-^{32}P]dCTP was purchased from Perkin-Elmer (Branchburg, NJ). TaqPro™ Complete DNA Polymerase mix, 2.0 mM $MgCl_2$ was received as a sample from Denville Scientific Inc. (Metuchen, NJ). MicroAmp reaction tubes were purchased from Applied Biosystems (Foster City, CA). Oligonucleotides were purchased from MWG Biotech (High Point, NC).

Yeast Strains:

Strain	Mating Type	Genotype	Plasmid
975	h^+	*wt*	
AP77	h^-	*ade1 ade6-M210 leu1 ura4*	
APP1	h^+	*ura4-D18 pcm2::ura4*$^+$	
CLP01	h^+	*leu1-32*	*pNMT:pcm2/Leu2*
FWP10	h-	*Wt*	
FWP16	h^+	*ura4-D18*	
KBP4 KBP5 KBP6 KBP7 KBP8	h^-	*ade1 ade6-M210 leu1-32 ura4-D18 pcm2::ura4*$^+$ *mutX*$^-$	*pNPT/ADE1-3/pcm2*
KHP01	h^+	*leu1-32 ura4-D18 pcm2::ura4*$^+$	*pNMT:pcm2/Leu2*
LNP25	h^-	*ade1 ade6-M210 leu1-32 ura4-D18 pcm2::ura4*$^+$	
LNP35t	h^-	*ade1 ade6-M210 leu1-32 ura4-D18 pcm2::ura4*$^+$	*pNPT/ADE1-3/pcm2*

Media:

Yeast were grown in various liquid and solid media, with compositions as follows:

YEL liquid: 5 g/L yeast extract, 2 g/L casamino acids, 30 g/L glucose

YEA solid: 5 g/L yeast extract, 2 g/L casamino acids, 30 g/L glucose, 20 g/L agar

YEA +adenine solid: YEA solid with 100 mg/L adenine

YEA +adenine +geneticin solid: YEA +adenine solid with 100 mg/L geneticin added after autoclaving and cooling

MEA solid: 30 g/L malt extract, 4 g/L glucose, 20 g/L agar

PM complete liquid: 3 g/L phthallic acid, 3.4 g/L sodium phosphate, 5 g/L ammonium chloride, 30 g/L glucose, 20 ml/L PM salts, 75 mg/L histidine, 75 mg/L uracil, 75 mg/L adenine, 150 mg/L leucine. The solution was brought to pH of 5.6 using 1 M KOH and autoclaved. After cooling, 1 mL/L PM vitamins and 0.1 mL/L PM minerals were added.

PM –leucine liquid: PM complete liquid without leucine

PM complete solid: 3 g/L phthallic acid, 3.4 g/L sodium phosphate, 5 g/L ammonium chloride, 30 g/L glucose, 20 ml/L PM salts, 75 mg/L histidine, 75 mg/L uracil, 75 mg/L adenine, 150 mg/L leucine, 20 g/L agar. The solution was brought to pH of 5.6 using 1 M KOH and autoclaved. After cooling, 1 mL/L PM vitamins and .1 mL/L PM minerals were added.

PM minimal liquid: PM complete liquid without histidine, uracil, adenine, leucine

PM minimal solid: PM complete solid without histidine, uracil, adenine, leucine

PM –uracil solid: PM complete solid without uracil

PM –leucine solid: PM complete solid without leucine

PM –leucine –adenine solid: PM complete solid without leucine or adenine

PM complete +geneticin solid: PM complete solid with 100 mg/L geneticin added after autoclaving and cooling

PM complete, pH 6.9, liquid: PM complete liquid, brought to a pH of 6.9 using 1 M KOH before autoclaving

PM -leucine, pH 6.9, solid: PM -leucine solid, brought to a pH of 6.9 using 1 M KOH before autoclaving

PM complete, 1 M KCl, liquid: PM complete liquid with 74.6 g/L KCl added with PM salts

PM -leucine, 1 M KCl, solid: PM -leucine solid with 74.6 g/L KCl added with PM salts

PM complete, 1.6 M sorbitol, liquid: PM complete liquid with 291.5 g/L sorbitol added with glucose

PM -leucine 1.6 M sorbitol, solid: PM -leucine solid with 291.5 g/L sorbitol added with glucose

PM salts: 53.5 g/L magnesium chloride, .75 g/L calcium chloride, 50 g/L potassium chloride, 2 g/L sodium sulfate. This solution was filter sterilized and stored at 4 ˚C.

PM vitamins: 1 g/L pantothenic acid, 10 g/L nicotinic acid, 10 g/L inositol, 10 mg/L biotin. This solution was filter sterilized and stored at 4 ˚C.

PM minerals: 5 g/L boric acid, 4 g/L manganese sulfate, 4 g/L zinc sulfate, 2 g/L ferrous chloride, 1.6 g/L molybdic acid, 1 g/L potassium iodide, .4 g/L copper sulfate, 1 g citric acid. This solution was filter sterilized and stored at 4 ˚C.

Liquid Cultures:

To obtain a log phase culture, the following procedure was followed: A single colony of cells was cultured in 3-5 mL of PM complete liquid media at 30 ˚C. This was left to grow overnight to a density of at least 10^7 cells/mL. The cells were counted in a hemacytometer and diluted to a density between 10^6 - 5 x 10^6 cells/mL in the appropriate liquid medium. Cultures were then incubated at 30 ˚C with constant shaking at 220 RPM until they reached the desired densities.

Mutagenesis:

Log phase cultures, grown with geneticin to ensure plasmid retainment, were counted in a hemacytometer and resuspended in 1.5 mL PM Complete liquid media to a concentration of 1.33 x 10^8 cells/mL. These cells were washed with 1 mL 10 mM KH_2PO_4, pH 7.0, and resuspended in 1.5 mL of this same buffer. A 1.0 mL aliquot of this was removed to a fresh tube and mixed with a specified amount of ethylmethanesulfate. The tube was shaken at 30 ˚C for various times as indicated in the text, after which a 0.25 mL aliquot of the solution was transferred to a new tube and mixed with 1 mL 5 % sodium thiosulfate to stop the reaction. The cells were centrifuged and washed twice with 1 mL sterile water and once with 1 mL YEA liquid media. Cells were counted with a hemacytometer. Specified dilutions of the cells were then plated on YEA solid media using glass beads.

Rapid Transformation of *S. pombe*:

A large patch of cells was grown on PM complete solid media at 30 ˚C. This patch was then scraped into a tube containing 2 μL plasmid (0.5 μg – 1 μg) and 0.3 mL of PLATE buffer (40.5 % PEG-4000; 10 mM Tris-HCl, pH 7.5; 100 mM LiAc; 1 mM EDTA, pH 8.0) and incubated overnight at room temperature. Settled cells were then plated onto the appropriate selective solid medium.

RNA isolation:

RNA was isolated by a modification of the procedure described by Schmitt et al (1990). Cells were centrifuged at 2000 g for 5 minutes and resuspended in 400 μL of AE buffer (50 mM Na acetate, pH 5.3; 10 mM EDTA). The suspension was transferred to a screw cap microfuge tube, along with a volume of small glass beads equal to the size of the pellet of cells. Forty μL of 10 % SDS and 440 μL of phenol were added, and the tube was immediately vortexed and incubated at 65 ˚C for 4 minutes. The cells were then placed on dry ice until phenol crystals formed. The suspension was separated by centrifuging at 13,000x g for two minutes. The upper, aqueous layer was transferred to a new tube, and two extractions were performed with 400 μL 1:1 phenol:chloroform, followed by an extraction with 400 μL chloroform. The RNA was precipitated by adding 40 μL 3 M Na acetate, pH 5.3, and 1 mL ice-cold 95 % ethanol. This was stored at –20 ˚C for at least 1 hour. The suspension was centrifuged at 4 ˚C for 15 minutes to pellet the RNA. The pellet was then washed with 500 μL ice-cold 80 % ethanol and resuspended in 20 μL RNase-free sterile water.

RNA electrophoresis and Northern blot:

The gel apparatus was rinsed with DEPC-treated water to inactivate any associated RNase. A gel was prepared containing 0.25 g agarose in 15.5 mL DEPC-treated water, plus 5 mL

5 X MOPS buffer (0.2 M MOPS, pH 7.0; 50 mM Na acetate; 5 mM EDTA, pH 8.0) and 4.42 mL formaldehyde. Each RNA sample was prepared by mixing 1 – 5 μL RNA (5 – 20 μg RNA) with 5 μL formamide, 2 μL formaldehyde, 1 μL 5 X MOPS buffer, and 1 μL 400 μg/mL ethidium bromide. The samples were incubated at 65 ˚C for 10 minutes and placed on ice. A 2 μL aliquot of sterile loading buffer (50 % glycerol; 1 mM EDTA; 0.4 % bromophenol blue; 0.4 % xylene cyanol) was then added to each sample and the gel was run using 1 X MOPS buffer as the running buffer.

RNA was transferred to a positively charged membrane using the PosiBlot 30 – 30 Pressure Blotter and Pressure Control Station. After transfer, the RNA was cross-linked to the membrane with 1200 μjoules of ultraviolet radiation. Hybridization probes were labeled by random priming, using the DECAprime II kit, with [α-^{32}P]dCTP. The reaction mixture was centrifuged through a ProbeQuant G-50 micro column to remove unincorporated nucleotides from the probe. The membrane was prepared for hybridization by incubating it in a hybridization tube for 1 hour at 65 ˚C, in prehybridization solution (0.5 M sodium phosphate pH 7; 1 mM EDTA; 7 % SDS, 1 % BSA fraction V, 100 μg/mL salmon sperm DNA). The probe was then added and the tube was incubated overnight at 65 ˚C. The membrane was then washed with wash buffer (40 mM sodium phosphate; 1 mM EDTA; 1 % SDS) twice for 15 minutes and twice for 60 minutes. The membrane was put in a film cassette with Kodak Biomat MS film and an intensifying screen, and the cassette was stored at –80 ˚C for three weeks. The film was then developed using the X-O-mat machine.

Chapter 3: Analysis of wild-type *S. pombe pcm2* RNA expression

Based on the evidence in other organisms that PIMT is important during stress conditions, as well as the evidence suggesting this so far in *S. pombe*, we expect *pcm2* expression to increase during stress conditions. Previous experiments in our lab used Northern blots to show that *pcm2* expression increases during stationary phase growth, as well as during heat or osmotic shock. My goal is to expand on these experiments by using Real-Time RT-PCR to quantitively analyze 975 (wild-type) *pcm2* expression during a wider range of stress conditions. Real-Time PCR is a useful technique because it makes it very easy either to compare expression of a single gene across many different samples or to analyze the expression of multiple genes using a single RNA sample. PCR mix can be purchased containing a dye, SYBR Green, that fluoresces when bound to double-stranded-DNA. Then, as amplification progresses during the PCR, there is more dsDNA for the SYBR Green to bind to, and total fluorescence increases. The Real-Time machine measures fluorescence at each cycle and displays the data in terms of relative fluorescence units. Levels of initial cDNA, and therefore initial RNA, present in samples are compared using the "threshold value," or the number of cycles necessary to get relative fluorescence at 10 times the baseline level. Thus, I expect to see lower threshold values for stress condition samples, meaning that they have more initial *pcm2* transcripts.

The main steps of this process are: 1) RNA extraction from yeast samples; 2) DNase treatment to remove genomic DNA contamination; 3) reverse transcriptase reaction; 4) Real-Time PCR reaction and analysis. Currently, steps 1-3 have been completed successfully, and I am still working on step 4.

RNA extraction:

I extracted RNA from strain 975 cells under each of the following conditions: log phase growth, stationary phase growth, short-term heat shock, long-term heat shock, 1.6 M sorbitol, 1 M KCl, and pH 6.9 (see Figure 2). Here, log phase growth was used as a control, and each of the stress condition cultures, except for the stationary phase culture, consisted of cells in log phase. The heat shock stress conditions were achieved by incubating the cultures at 37 ˚C instead of at 30 ˚C – the long-term heat shock culture was placed at 37 ˚C from the very beginning of the starter culture, while the short-term heat shock culture was placed at 37 ˚C for only 1 hour before the extraction. The 1.6 M sorbitol, 1 M KCl, and pH 6.9 stress conditions were achieved by incubating cells in PM complete media with these additions. The extraction was performed as described. Spectrophotometer readings at 260 nm were used to determine the concentrations of RNA in the various extracts. The samples were run on a denaturing gel as described to confirm the presence of RNA and its integrity (see Figure 3). The apparent sizes of the ribosomal RNA bands for all seven samples agree nicely with the published rRNA sizes of 3.5 and 1.8 kb.

The amount of RNA extracted from each cell ranged from $5.47 * 10^{-8}$ – $4.94 * 10^{-7}$ μg. This is much less than the known RNA content for a yeast cell, which is approximately 3 pg, or $3 * 10^{-6}$ μg. The basis for the low efficiency of the extraction is not known. The poor yield could be due to the toughness of the yeast cell wall. Even though hot phenol and glass beads are used in the extraction to break through the cell wall, these extreme treatments may not be sufficient to disrupt all cells. If fewer than all of the cells are broken up, the amount of RNA extracted will be lower than expected. Yeast cells in stationary phase have particularly tough cell walls, as the cells are not dividing in stationary phase. This may explain why the yield of RNA from the

Figure 2

sample condition	media (all are liquid)	temperature (ÞC)	density of culture (cells/mL)	# cells used for extraction	total RNA extracted (µg)	RNA extracted per cell (µg/cell)
log phase	PM complete	30	$8.25 * 10^{6}$	$3 * 10^{8}$	91.2	$3.04 * 10^{-7}$
stationary phase	PM complete	30	$1.41 * 10^{8}$	$3 * 10^{8}$	16.4	$5.47 * 10^{-8}$
1.6 M sorbitol	PM complete +1.6 M sorbitol	30	$7.83 * 10^{6}$	$3 * 10^{8}$	104.8	$3.49 * 10^{-7}$
1 M KCl	PM complete +1 M KCl	30	$5.8 * 10^{6}$	$8.64 * 10^{7}$	31.1	$3.60 * 10^{-7}$
pH 6.9	PM complete pH 6.9	30	$8.17 * 10^{6}$	$3 * 10^{8}$	148.2	$4.94 * 10^{-7}$
heat shock – long term	PM complete	37	$1.27 * 10^{7}$	$3 * 10^{8}$	139.8	$4.66 * 10^{-7}$
heat shock – short term	PM complete	30, moved to 37 for 1 hour before extraction	$1.3 * 10^{7}$	$3 * 10^{8}$	81	$2.7 * 10^{-7}$

Summary of RNA extractions from wild type (strain 975) cells at various conditions.

Figure 3

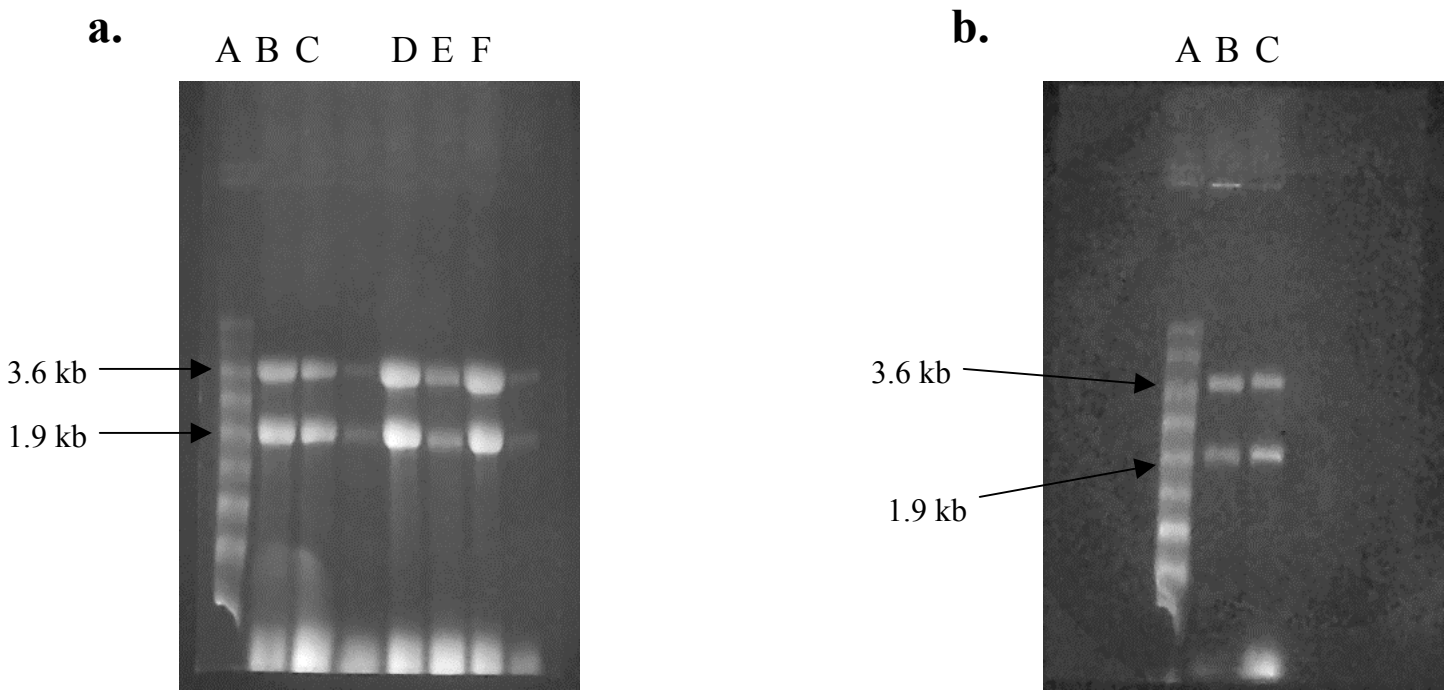

RNA extracted from 975. a) Lane A -standard marker; Lane B - log phase growth; Lane C - heat shock, short-term; Lane D - 1.6 M sorbitol; Lane E - 1 M KCl; Lane F - pH 6.9; **b)** Lane A - standard marker; Lane B - stationary phase growth; Lane C - heat shock, long-term

stationary phase sample is a full order of magnitude lower than the yields for all of the other log phase samples.

DNase treatment:

After an RNA extraction, there is frequently some amount of genomic DNA left in the solution of RNA. Even small amounts of genomic DNA can obscure the PCR results of the cDNA you actually want to amplify. I used the DNA-*free*™ DNase treatment kit, which consists of a treatment buffer, a DNase, and a DNase-inactivation reagent, to treat each of my samples. The samples in Figure 3 were analyzed prior to DNase treatment. The presence of high-molecular-weight material in the samples in panel b is consistent with some DNA contamination in the stationary phase and long-term heat shock samples. The absence of such high-molecular-weight bands in panel a does not exclude possible DNA contamination. Therefore, I treated 1-3 μL of each RNA sample with DNase, to yield final DNA-free RNA solutions with concentrations ranging from 0.084 – 0.15 μg/μL.

Reverse transcriptase reaction:

I used the iScript cDNA synthesis kit to reverse-transcribe the RNA into cDNA. This kit consists of a reaction mix, containing buffer, nucleotides, and oligo and hexamer random primers, and a reverse transcriptase. I used 1 μg of RNA in each sample, including a control reaction, which lacked reverse transcriptase, for each sample.

Real-Time PCR:

Primers for the RT-PCR, SP24 and SP25, were designed using the Beacon Designer 2 program (Premier Biosoft International; Palo Alto, CA). The expected product size with these primers is 188 bp. The forward primer, SP24, has a sequence of

5’-ACGAATCAGAGAGCCATCAAG-3’.The reverse primer, SP25, has a sequence of 5’- CCAATATCCAAGGCAGAACAG-3’.

The first step to this was to determine an optimal PCR protocol. To do this, I ran a normal PCR on two RT samples – log phase growth and heat shock, long-term – as a text. I set up each reaction using the TaqPro PCR mix according to manufacturer’s instructions and the SP24 and SP25 primers at a final concentration of 2 μM, along with 1 μL of the RT sample. For the amplification, I used a 5 minute initial denaturation, forty amplification cycles (95 ˚C-1 min., 55 ˚C-2 min., 72 ˚C-3 min.), and a final extension at 72 ˚C for 7 minutes. Electrophoresis on a 1.5 % agarose gel confirmed that a product of the correct size was formed in each reaction.

Once I knew that these conditions did allow for amplification by these primers, I did two runs of Real-Time PCR on my RT samples. In addition to running PCR reactions of my samples, I did several controls: a positive control, using the plasmid *pNPT/ADE1-3/pcm2*; a negative control, with water in place of any sample; seven more negative controls, in which reverse transcriptase had been omitted (in the first run, I used only the –RT log phase growth control; in the second run, I used all –RT samples). I set up reactions using the iQ SYBR Green Supermix according to manufacturer’s instructions and the SP24 and SP25 primers at a final concentration of 2 μM. I used the same PCR protocol as above (see Figure 4.a), and following the Real-Time PCR, I ran an aliquot of each sample from the PCR well on a 1.5 % agarose gel to confirm the Real-Time results (see Figure 4.b).

Figure 4

a.

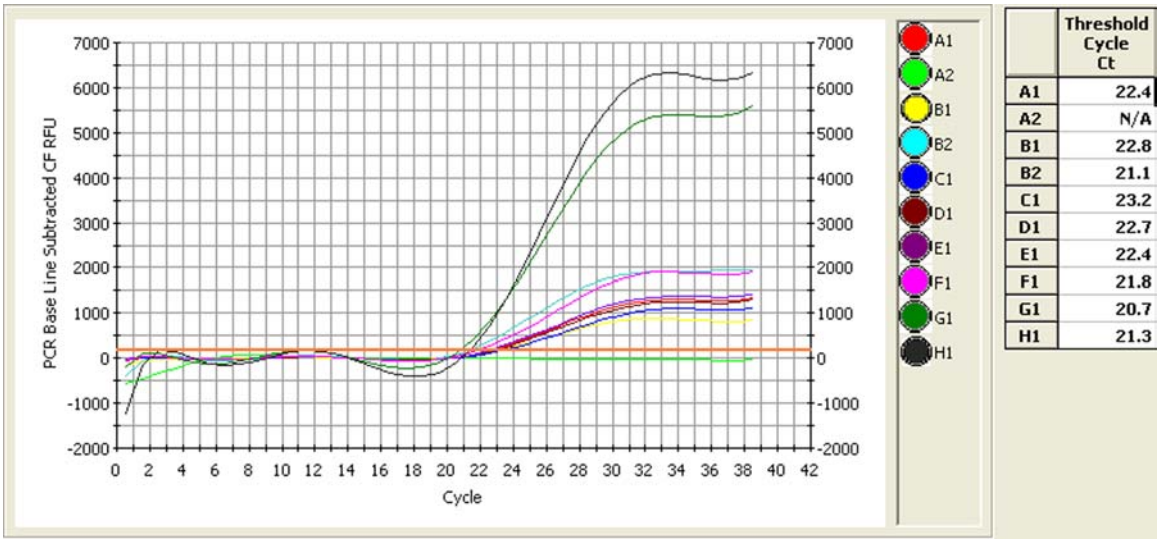

	Threshold Cycle Ct
A1	22.4
A2	N/A
B1	22.8
B2	21.1
C1	23.2
D1	22.7
E1	22.4
F1	21.8
G1	20.7
H1	21.3

b.

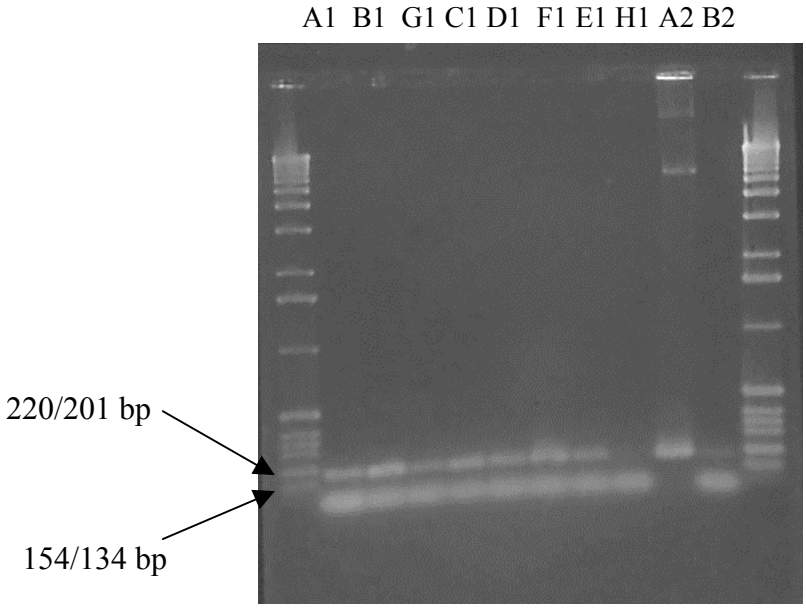

Real-Time PCR summary. a) # of cycles vs. relative fluorescence units with baseline amounts subtracted; table of threshold values; **b)** gel of samples (standard marker X is seen on both ends of the gel)

A1 - log phase growth, **A2** - plasmid control, **B1** - stationary phase growth, **B2** - water control, **C1** - heat shock short-term, **D1** - 1.6 M sorbitol, **E1** - pH 6.9, **F1** - 1 M KCl, **G1** - heat shock long-term, **H1** - -RT log phase growth control

I expected the two negative controls (water and –RT) to have the least amplification and therefore the highest threshold values, the positive control (*pNPT/ADE1-3/pcm2*) to have the most amplification and the lowest threshold value, and the seven samples to have amplification and threshold values in between those of the negative and positive controls. However, according to the Real-Time data, the positive control plasmid sample had the least amplification, indeed, showing almost none at all. The –RT log phase growth control sample showed the most amplification. Each of the other samples was somewhere in between, but for six of the seven RT samples, amplification was quite low. Also, the threshold cycle value for each sample was very similar, with all threshold cycle values ranging only from 20.7-23.2, except for the plasmid control, which was not assigned a threshold cycle value.

On the other hand, according to the gel, the plasmid sample certainly had a lot of amplification, while the –RT control had practically none. Each of the seven RT sample lanes also showed a product band. Since, for example, the sample with the lowest amplification according to the Real-Time data (plasmid control) was taken directly from that well and run on a gel, where it showed a significant DNA band, I know that the Real-Time output is incorrect. I hypothesize that the Real-Time machine was either misreading the fluorescence or misinterpreting the data. When the Real-Time PCR was repeated, similar results were obtained. This leaves me with no usable results on the relative expression of *pcm2* during various stress conditions. I am currently in the process of working out this problem.

Chapter 4: Effects of loss of *pcm2* in *S. pombe*

As discussed earlier, loss of PIMT is known to cause observable phenotypic changes in several organisms, including *E. coli*, *C. elegans*, and mice. Phenotypes appear when the organism is under stress conditions. Earlier work in our lab established that loss of PIMT activity did not affect vegetative growth in yeast. My goal is to determine the effect of PIMT loss on cell growth and viability under various stress conditions. For these experiments, I chose to use spot plates to assess viability. Spot plates are useful because they allow you to compare growth of several strains on the same plate. Viability is assessed by qualitatively comparing spot density and size, rather than counting individual cells or comparing growth in streaks. I also kept records of cell growth/viability by taking pictures of the plates.

Stationary Phase Survival:

Work from other organisms suggested that PIMT deficiency might reduce the ability of cells to survive in stationary phase. In this new experiment, relative cell viability was determined by plating cells at various timepoints after they entered stationary phase.

I first compared the survival of the *pcm2*-knockout strain, APP1 (*ura4-D18; pcm2::ura4*$^{+}$), to that of the wild-type strain FWP10 and that of FWP16 (*ura4-D18*), the parental strain for APP1. For each yeast strain, starter cultures were initially diluted in PM Complete liquid media to give a 10 mL culture with cell density of $2 * 10^6$ cells/mL. One culture was then incubated continuously at 30 ˚C and the other was incubated at 36 ˚C, with constant shaking. Cells in all cultures entered stationary phase within the first day of incubation. Cell densities ranged from $7.7 * 10^7 – 1.76 * 10^8$ initially and stayed more or less constant throughout the experiment.

Viability was assessed every day for the 36 ˚C cultures, and on days 1, 7, 10, and then every other day for the 30 ˚C cultures. To assess viability, cultures were first counted in triplicate in the hemacytometer to obtain cell density. Then, a series of 1:5 dilutions was prepared in PM Complete liquid media, such that the first dilution contained $1 * 10^7$ cells/mL (experiment 1) or $2 * 10^7$ cell/mL (experiment 2), and the final dilution contained $1.6 * 10^4$ cells/mL (experiment 1) or $1.28 * 10^3$ cells/mL (experiment 2). An aliquot of each dilution (10 μL for experiment 1, 5 μL for experiment 2) was plated on YEA solid media, and the plates were then incubated at 30 ˚C. After three days of growth, pictures were taken of the plates.

The first run of this experiment (see Figure 5.a) showed that at 36 ˚C, some cells from all three strains were still viable at 4 days, but no viable cells remained at 5 days. At 30 ˚C (see Figure 6.a), FWP16 cell viability was lost by 26 days. By day 32, APP1 cell viability was also lost, and only a few viable FWP10 cells were remaining. FWP16 probably lost viability first because it is a uracil auxotroph, while both APP1 and FWP10 have functional $ura4^+$ genes. Thus, the first experiment indicates that, compared to the wild-type control FWP10 strain, loss of *pcm2* does not negatively affect the viability of APP1 in stationary phase at 36 ˚C, but may slightly reduce the viability of APP1 at 30 ˚C.

When the experiment was repeated, FWP16 cells lost viability between 3 and 5 days at 36 ˚C, while FWP10 and APP1 cells lost viability between 5 and 7 days (see Figure 5.b). At 30 ˚C, a loss in FWP16 viability was apparent at 20 days, and no viable FWP16 cells remained at 30 days. The loss of viability of wild-type and knockout cells occurred later, such that no viable FWP10 or APP1 cells were detected at 34 or 36 days, respectively (see Figure 6.b). As in the first experiment, FWP16 probably lost viability first because of its inability to synthesize uracil,

Figure 5

a.

APP1

FWP10

FWP16

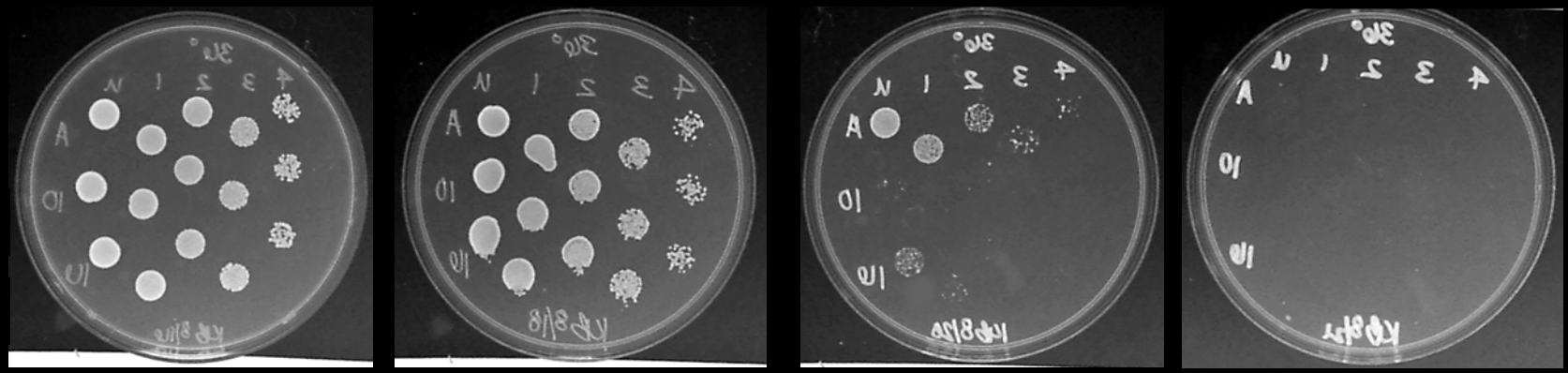

Day 0 Day 2 Day 4 Day 5

b.

FWP10

FWP16

APP1

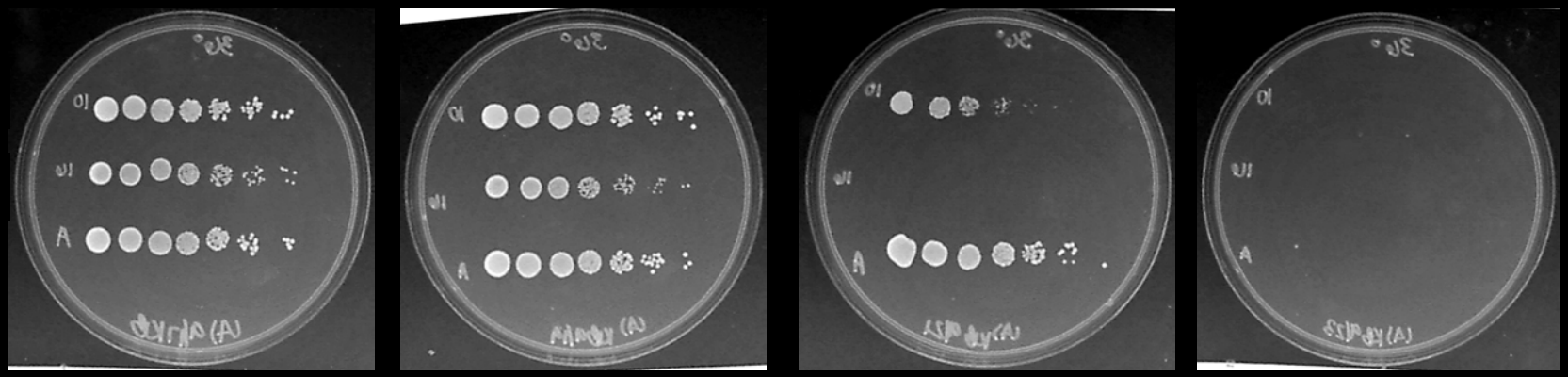

Day 1 Day 3 Day 5 Day 7

Stationary phase survival of APP1, FWP10, and FWP16 at 36 ˚C. (a) first experiment - top line: APP1, middle line: FWP10, bottom line: FWP16, **(b)** second experiment - top line: FWP10, middle line: FWP16, bottom line: APP1

Figure 6

a.

APP1

FWP10

FWP16

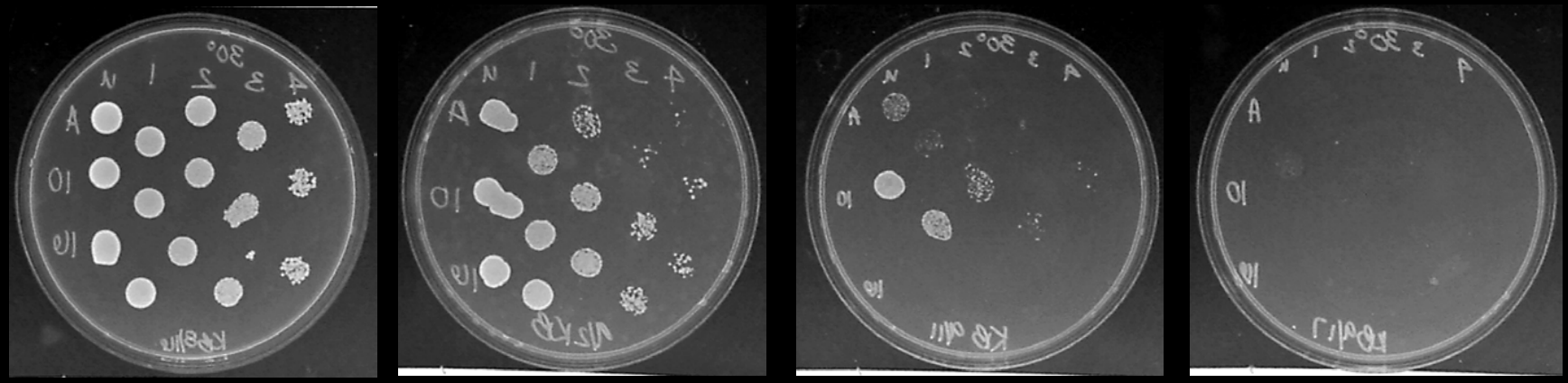

Day 0 Day 17 Day 26 Day 32

b.

FWP10

FWP16

APP1

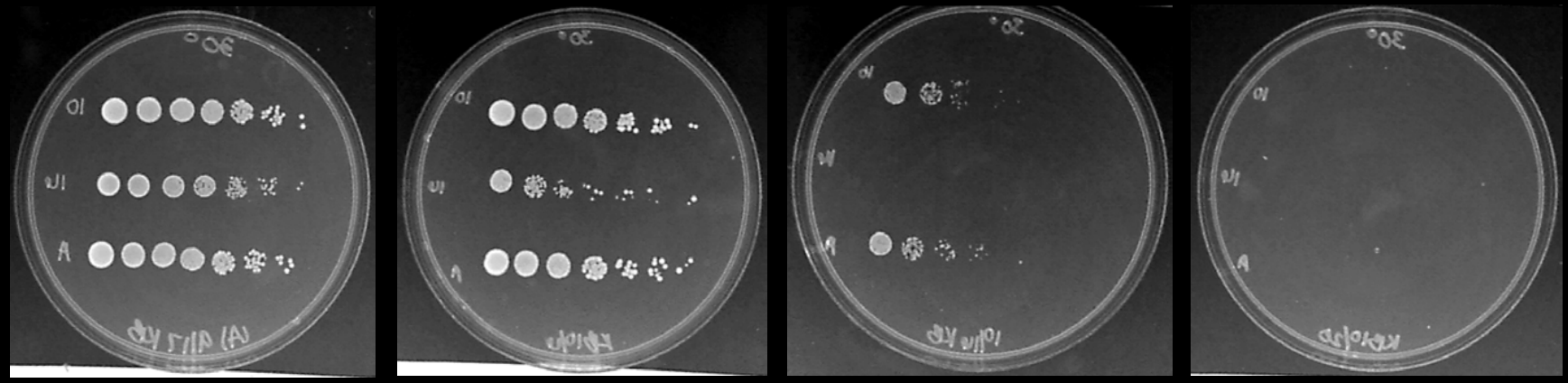

Day 1 Day 20 Day 30 Day 34

Stationary phase survival of APP1, FWP10, and FWP16 at 30 ˚C. (a) first experiment - top line: APP1, middle line: FWP10, bottom line: FWP16, **(b)** second experiment - top line: FWP10, middle line: FWP16, bottom line: APP1

and loss of *pcm2* did not affect viability at 36 ˚C. In contrast to the first experiment, however, APP1 survived slightly longer in stationary phase at 30 ˚C than FWP10 did.

These two experiments fail to show a significant, reproducible difference in the survival of APP1 and FWP10 in stationary phase. Because of this, I conclude that loss of *pcm2* does not directly affect survival of yeast in stationary phase, either at 30 ˚C or at the stress temperature of 36 ˚C.

Stress Condition Survival:

I also used the spot plate method to compare APP1 survival under various stress conditions to that of wild-type strain 975 and to two Pcm2p-overexpressing strains, CLP01 and KHP01. Strains CLP01 and KHP01 were constructed by transforming a *pNMT:pcm2/Leu2* plasmid into strains with wild-type or nonfunctional *pcm2* genes. Here I hypothesized that APP1 would grow less well than strain 975 under stress conditions, and that the overexpression strains would grow as well or better than strain 975.

In the first experiment, I grew cultures of APP1, 975, and CLP01 (*leu1-32;pNMT:pcm2/Leu2)* in PM -leucine liquid media to mid-log phase. Cell densities were determined by counting in the hemacytometer and spot plates were done on control PM –leucine media, as well as on a variety of the same media modified to induce stress responses. Modified media contained 1.6 M sorbitol, 1 M KCl, or additional base to bring the pH to 6.9. Each spot plate contained a 10-fold dilution series for each strain, with cell numbers ranging from $1.2 * 10^4$ cells/spot to 12 cells/spot. Duplicate plates were incubated for three days at 30 ˚C and 37 ˚C. The 37 ˚C plates add a second stress associated with high temperature (see Figure 7).

There was very little difference in growth between APP1 and 975 cells on all plates. On the other hand, CLP01 grew consistently less well than the other two, despite its increase in

Figure 7

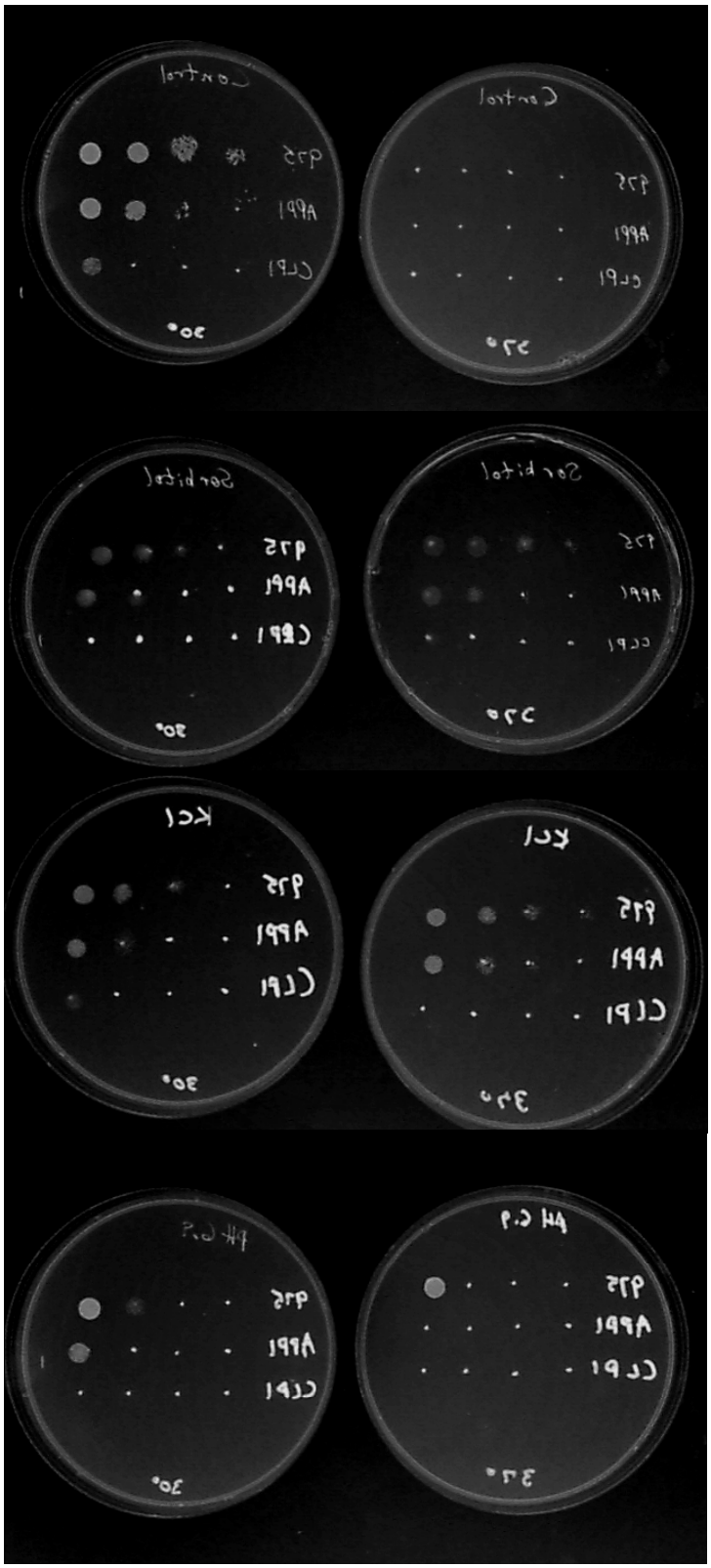

Growth of 975, APP1, and CLP01 under various stress conditions, at 30 ˚C (left) and 37 ˚C (right). On each plate, the top row of spots is 975, the middle row is APP1, and the bottom row is CLP01.

pcm2 expression. It is not clear if the reduced viability of CLP01 is related to leucine auxotrophy or to high levels of protein expression from the plasmid.

There were also several interesting results unrelated to the level of *pcm2* expression. Surprisingly, cells grew better at 37 ˚C in the presence of either 1.6 M sorbitol or 1 M KCl, suggesting some crossprotection from osmotic and heat shocks. Growth at pH 6.9 was only detected in cells at high density, suggesting that metabolic byproducts may condition the media locally, allowing growth to occur there.

The experiment in Figure 7 was repeated with a new overexpressing strain, KHP01, which displayed better growth properties than CLP01 under permissive conditions. The endogenous *pcm2* gene of KHP01 had been replaced with a ura4^{+} gene. In the second experiment, cultures of 975, APP1, and KHP01 (*ura4-D18;leu1-32;pcm2::ura4+; pNMT:pcm2/Leu2*) were grown in PM –leucine liquid media to mid-log phase. Densities were determined with the hemacytometer and spot plates on the same control and stress media were done using a 10-fold dilution series, with cell numbers ranging from 1.07 * 10^4 cells/spot to 10 cells/spot. The plates were also incubated at both 30 ˚C and 37 ˚C for three days (see Figure 8).

The results in the second experiment are almost identical to those from the first experiment. These plates once again show similar growth between strains APP1 and 975. Strain KHP01 grew less well than the other two, suggesting that the reduced growth is not due to differences in genetic background between CLP01 and KHP01.

Both experiments fail to show any difference in growth between *pcm2*-knockout APP1 and wild-type 975 under stress conditions. These results suggest either that *pcm2* is not involved in stress responses or that *S. pombe* may carry a second gene that compensates for loss of *pcm2*.

Figure 8

Control

1.6 M Sorbitol

1 M KCl

pH 6.9

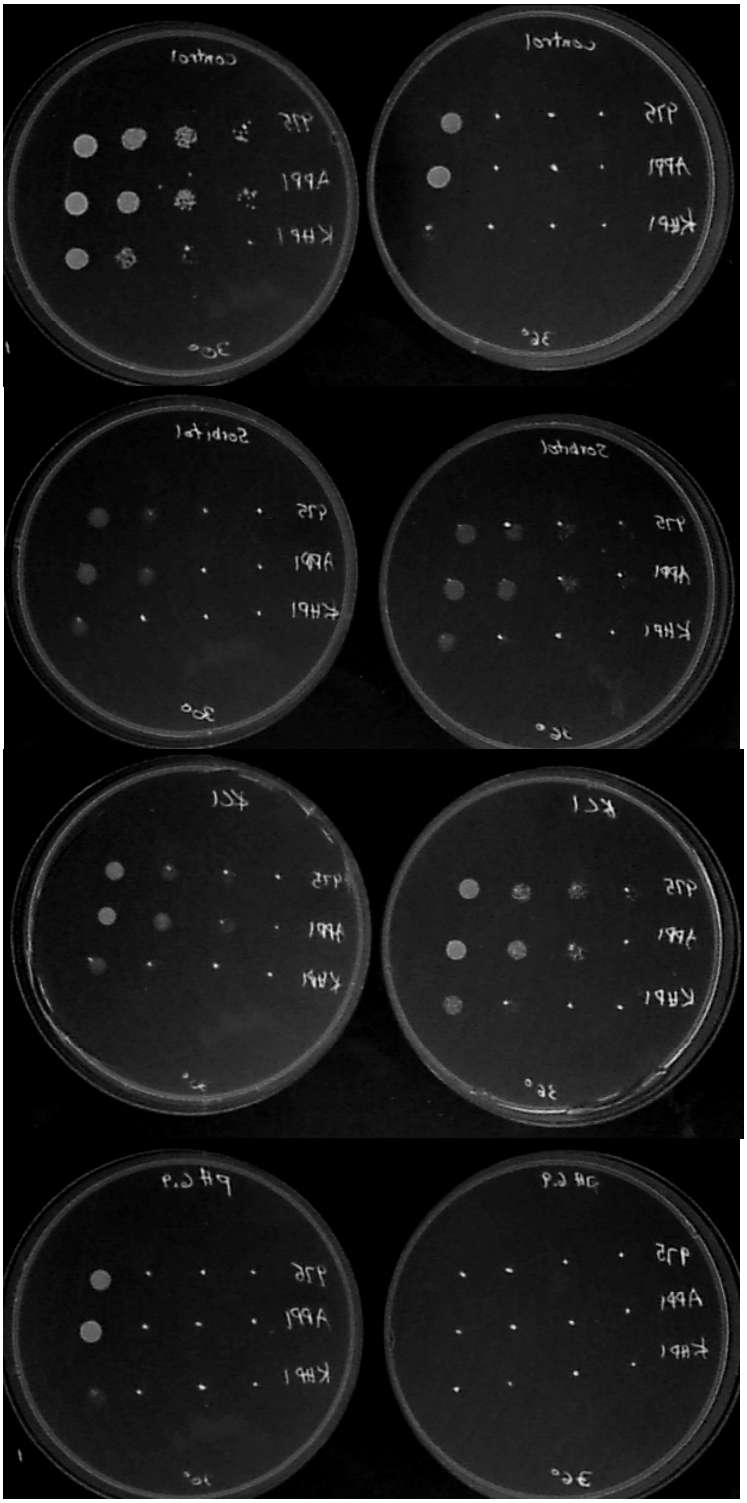

Growth of 975, APP1, and KHP1 under various stress conditions, at 30 ˚C (left) and 37 ˚C (right). On each plate, the top row of spots is 975, the middle row is APP1, and the bottom row is KHP1.

Chapter 5: Synthetic Lethal Screen

Since no phenotype has been identified yet for strains lacking *pcm2*, we hypothesize that there may be other genes whose products compensate for the loss of Pcm2p. My goal is to identify this gene or genes with a synthetic lethal screen. The main steps of this screen are: 1) creation of a *pcm2*-knockout yeast strain with appropriate markers; 2) transformation of this strain with a *pcm2*-carrying plasmid; 3) mutagenesis of this transformed strain; 4) screening of mutagenized cells for potential synthetic lethal strains; 5) backcrossing synthetic lethal strains into a uniform genetic background; 6) identification of mutant alleles by complementation. Currently, steps 1-4 have been performed. I am in the process of repeating steps 3 and 4 to get a few more potential synthetic lethal strains before moving on to step 5.

Previously, a strain for mutagenesis, LNP35t, was constructed (step 1). To do this, APP1, the *pcm2*-knockout strain, was mated with AP77 to introduce selective markers. The resulting strain, LNP25, was transformed with the *pNPT/ADE1-3/pcm2* plasmid (step 2), to give LNP35t.

Confirmation of *pcm2* expression in LNP35t:

The success of the synthetic lethal screen is dependent upon successful production of Pcm2p in LNP35t. It is also critical that the only source of Pcm2p is the *pNPT/ADE1-3/pcm2* plasmid. Our lab has previously shown that APP1 lacks *pcm2* transcripts (Northern, unpublished data). Since APP1's *pcm2::ura4+* mutation was selected for in the mating that produced LNP35t, we know that LNP35t lacks a genomic copy of *pcm2*. Thus, my first goal was to show that LNP35t produces *pcm2* transcripts, which we would assume to be coming from the plasmid. This would ensure that both of the above-mentioned conditions were met before beginning the mutagenesis.

To verify *pcm2* expression, I did a Northern blot of RNA extracted from both log and stationary phase LNP35t cells. Cultures of LNP35t were grown in PM complete liquid media at 30 ˚C to a density of 3.75 * 10^6 cells/mL for the log phase culture and 8.8 * 10^7 cells/mL for the stationary phase culture. Suspensions of 9 * 10^7 and 1.8 * 10^8 cells for the log and stationary phase cultures, respectively, were used for RNA extraction. The RNA was run on a denaturing gel and blotted to a nylon membrane as described (see Figure 9). Finally, a probe for *pcm2* was hybridized to the membrane, which was exposed to film and developed. Transcripts for *pcm2* were detected in both the LNP35t log phase (Lane A) and LNP35t stationary phase (Lane B) lanes, showing the *pNPT/ADE1-3/pcm2* does, indeed, provide a functional source of Pcm2p.

Previous experiments have shown that endogenous *pcm2* transcription is increased in stationary phase cells relative to log phase cells (Northern, unpublished data). In this experiment, much less total RNA was present in the LNP35t stationary phase lane than in the LNP35t log phase lane, as seen on the gel. The Northern blot reflects this same relative level of *pcm2* expression, as there was less *pcm2* transcript detected in the stationary phase lane. This suggests that unlike the endogenous transcript, plasmid-encoded transcripts are not present at higher levels in stationary LNP35t cells than in log LNP35t cells. This further suggests that the regulation of the plasmid-encoded *pcm2* gene is not identical to that of the native gene, even though flanking regions were cloned into the *pNPT* vector.

Mutagenesis of LNP35t:

For a synthetic lethal screen, optimal results are expected when approximately 60% of cells are killed by the mutagen. This is achieved by adjusting the length of time of mutagenesis and/or the amount of mutagen used. The first step of the mutagenesis was to run several trials to determine the correct parameters. I used a constant 20 μL dose of ethylmethanesulfate (EMS) for

Figure 9

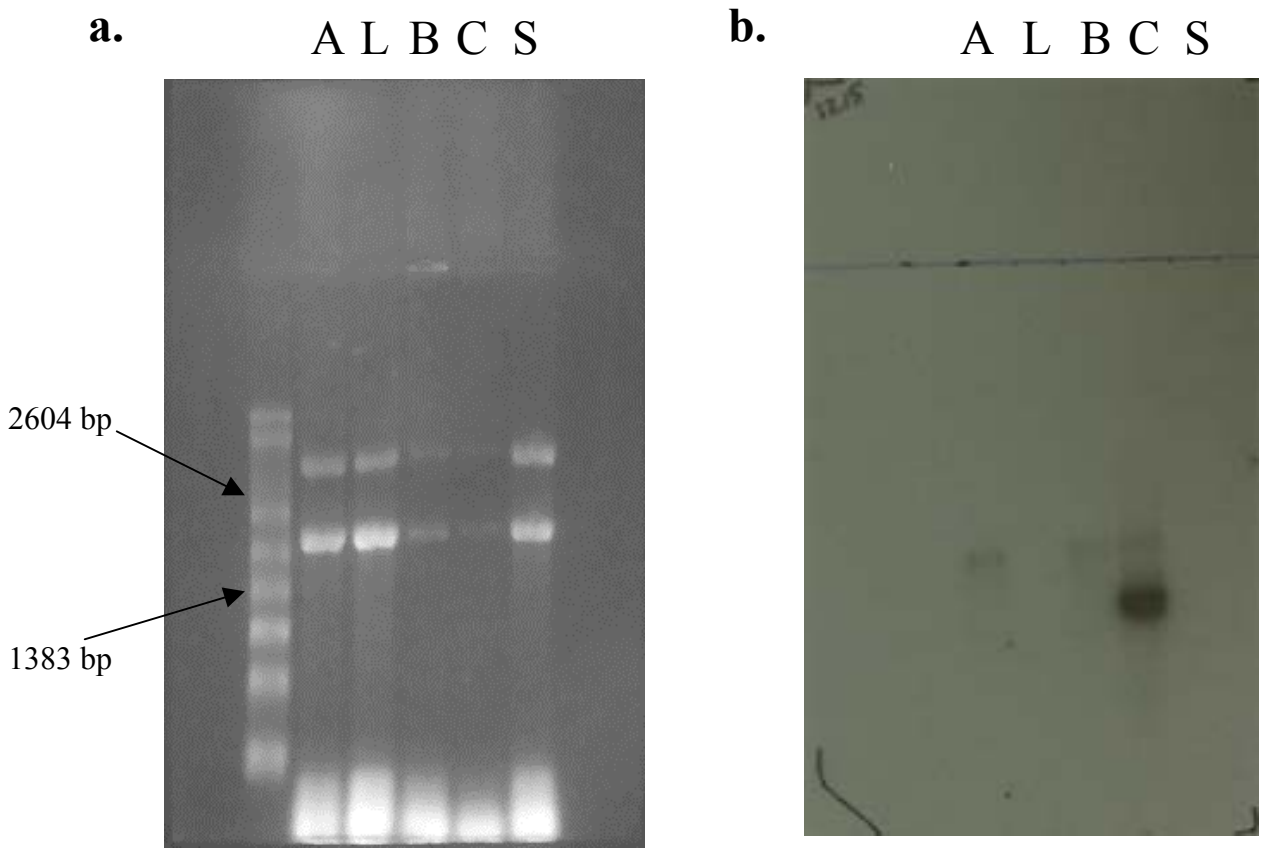

Presence of *pcm2* transcripts in LNP35t and CLP01 cells. a) denaturing agarose gel of extracted RNA, with Standard Markers in first lane; **b)** Northern blot of gel

Lane A: LNP35t log phase cells, showing *pcm2* transcripts from *pNPT/ADE1-3/pcm2*
Lane L: 975 log phase cells
Lane B: LNP35t stationary phase cells, showing *pcm2* transcripts from *pNPT/ADE1-3/pcm2*
Lane C: CLP01 stationary phase cells, showing *pcm2* transcripts from *pNMT:pcm2/Leu2*.
Lane S: 975 stationary phase cells

a 1 mL aliquot of approximately 1.33 * 10^8 cells, and performed rounds of mutagenesis for various times. The percent killing was determined by comparing the number of living cells after mutagenesis (as determined by counting colonies in plated dilutions) to the initial number of cells mutagenized, and adjusting for random killing with a negative control group of cells that went through the whole procedure without EMS exposure. After trying timepoints varying from 30-120 minutes, I determined that 30 minutes was the optimal time to use for approximately 60% killing. After this, the percent killing was evaluated following each round of mutagenesis, and the amount of EMS used was varied as needed (up to 40-50 μL) each time to obtain 60 % killing.

Several rounds of mutagenesis were then performed on LNP35t log phase cultures (see Figure 10). Mutagenized cells were then plated on YEA solid media and grown at the stress temperature of 37˚C for 3-4 days. This temperature was chosen for screening because *pcm2* transcription in *S. pombe* increases at elevated temperatures, possibly reflecting an increased importance of *pcm2* at high temperatures. We hypothesize that there is an increased possibility of isolating a synthetic lethal mutant at elevated temperatures.

Screening of Mutagenized Cells:

This screen takes advantage of properties of the adenine biosynthetic pathway, which contains two key genes, *ade1* and *ade6*. When cells grow on media that has little or no adenine, both of these genes become active. The *ade1* gene product produces a red intermediate that the *ade6* gene product converts into a colorless product. If both genes are functional, the path will run all the way through, and the cells will appear white in color. The cells will also appear white if they are *ade1*-deficient because no red intermediate will ever be made. However, cells that are *ade1+ ade6-* will build up the red intermediate and appear red. LNP35t is *ade1+ ade6-*, so it grows red on YEA plates, which have low amounts of adenine. However, since YEA plates

Figure 10

Experiment	EMS (uL)	Killing (%)	Total colonies screened	Mutants from 1˚ screen	Mutants from 2˚ screen	Potential synthetic lethals
A	40	29.0	62,300	2	2	KBP4 KBP5
B	45	37.6	29,100	1	0	
C	50	95.4	5,760	4	0	
D	45	62.4	24,300	10	2	KBP6 KBP7
E	45	67.8	43,500	32	6	KBP8

Summary of mutagenesis performed on LNP35t

aren't selective (i.e. don't contain geneticin), LNP35t can throw out the *pNPT/ADE1-3/pcm2* plasmid, which then makes the cells *ade1-ade6-* and white in color. As some individual cells in a colony throw out the plasmid while others don't, this causes red and white patches within single colonies. Colonies that do this are said to sector.

The synthetic lethal screen assumes that if the cells need either *pcm2* or a compensating gene to survive, and the mutagen causes a mutation in the compensating gene, the mutated cells will then require the presence of the *pNPT/ADE1-3/pcm2* plasmid to encode functional *pcm2*. If the cells can no longer throw out the plasmid because they rely on it for survival, they will not sector. Thus, mutagenized cells grown on YEA media were screened for colonies that appeared unable to sector.

Any colony that appeared uniformly red was streaked onto a fresh YEA plate and incubated at 37 ˚C for 3-4 days. Two additional rounds of screening were done to ensure that non-sectoring colonies were homogeneous. Currently, after screening approximately $1.65 * 10^5$ colonies, I have identified five such strains, KBP4-8 (see Figure 10). I am in the process of performing more rounds of mutagenesis to identify more potential synthetic lethal strains.

Testing of potential synthetic lethal strains:

The next step is to do a "plasmid shuffle," or to transform KBP4-8 with a second plasmid (*pNMT:pcm2/Leu2)* which also contains functional *pcm2*, and has *Leu2* as the selective marker. I then select for strains that lose the *pNPT/ADE1-3/pcm2* plasmid while retaining the *pNMT:pcm2/Leu2* plasmid. The purpose of the shuffle is two-fold. First, it ensures that the *pNPT/ADE1-3/pcm2* plasmid has not integrated itself into the genomic DNA. If it had, the cells would be unable to sector and would have been identified falsely as potential synthetic lethals. The easiest way to test for this is to look for the plasmid to be thrown out. However, if the strain

is actually a synthetic lethal strain, the cells won't be able to lose the *pNPT/ADE1-3/pcm2* plasmid unless they get another source of *pcm2* or the compensating gene. This leads to the second reason for the plasmid shuffle: it also ensures that the cells' inability to sector was actually due to a dependence on *pcm2* expression, and not on some other mutation. For example, a mutation that changes cell membrane permeability might make cells unable to lose plasmids. If the cells' reliance on the *pcm2* gene in *pNPT/ADE1-3/pcm2* was the only reason why they didn't sector, the *pcm2* gene in *pNMT:pcm2/Leu2* should be able to sustain them as well. Thus, potential synthetic lethal cells transformed with the *pNMT:pcm2/Leu2* plasmid should be able to sector on PM –leucine plates lacking adenine.

The *pNMT:pcm2/Leu2* plasmid was constructed previously in our lab (Levasseur and Heinecke, unpublished data). Since the success of this plasmid shuffle depends on the production of *pcm2* by this plasmid, my first step was to show that *pNMT:pcm2/Leu2* does indeed provide *pcm2* transcripts. I did this by doing a Northern blot of RNA extracted from a strain that carries the plasmid, CLP01 (*leu1-32; pNMT:pcm2/Leu2)*.

A culture of CLP01 was grown in PM –leucine liquid media at 30 ˚C to a density of $6.73 * 10^7$ c/mL. A suspension of $1.8 * 10^8$ cells was used for RNA extraction. The RNA was run on a denaturing gel and blotted to a nylon membrane as described. Finally, a probe for *pcm2* was hybridized to the membrane, and autoradiography was used to identify *pcm2* transcripts. Pcm2p encoding RNA was detected in the CLP01 lane (see Figure 9). Because only the coding sequence of *pcm2* was cloned into the *pNMT* vector, the expected transcript size is approximately 900 bp, considerably smaller than that expected for the *pNPT* insert, which included much of the *pcm2* 5' and 3' flanking regions, including three potential polyadenylation sites. Because the larger insert was used for the *pNPT* clone, the transcript may be closer to the

1.2 kb size of the major endogenous transcript, as determined previously in our lab (Northern, unpublished data). The CLP01 band shows large amounts of RNA detected, which makes sense because transcription of the *pNMT:pcm2/Leu2* DNA is driven by the powerful *pnmt41* promoter, which causes overexpression with an induction ratio of approximately 25 times (Forsburg 1993).

This blot also contained two lanes of strain 975 wild-type RNA, one from log phase (Lane L) and one from stationary phase (Lane S). The blot exposure was not long enough to detect endogenous *pcm2* RNA in either lane, while it was long enough to detect products from both plasmids in the other lanes. This indicates that the plasmids are very active. While I would have liked to see endogenous RNA in the wild-type lanes, the purpose of this experiment was to show *pcm2* expression from both plasmids, and this blot clearly does this.

Once I knew that *pNMT:pcm2/Leu2* does make Pcm2p, I could begin the plasmid shuffle. Potential synthetic lethal strains are being transformed with *pNMT:pcm2/Leu2* using the rapid transformation method as described. Strains are then screened for their ability to survive with only the *pNMT:pcm2/Leu2* plasmid. This screening is done by streaking transformed cells (those that grow on –leucine plates) onto PM –leucine –adenine plates and looking for streaks that sector. I have successfully transformed KBP4 and KBP5 and am in the process of screening transformants on PM –leucine –adenine plates. I am also in the process of transforming KBP6-8.

Chapter 6: Discussion and Future Work

One of the goals of my project was to study the effect of Pcm2p expression on stress responses and to determine if changes in *pcm2* expression occurred when cells were subjected to stresses. I tested the knockout strain APP1 under various conditions in search of a phenotypic effect associated with loss of *pcm2*. Long-term stationary phase growth at both 30 ˚C and 36 ˚C showed no consistent difference between APP1 and the control FWP10. Growth in high salt, high sugar, and high pH conditions at both 30 ˚C and 37 ˚C also showed no difference between APP1 and wild-type 975.

Unfortunately, I was unable to determine if stress treatments led to changes in *pcm2* gene transcription, as measured with Real-Time PCR. I successfully extracted RNA from *S. pombe* cultures during log phase growth and under six different stress conditions. Gel analysis of the samples after Real-Time PCR confirmed that the PCR had worked correctly, but that the results had either not been accurately recorded or accurately analyzed. In these experiments, the Real-Time data and threshold values did not agree with the more qualitative data obtained from the gel. Thus, I cannot yet make any conclusions about the relative expression of *pcm2* during different stress conditions. More work needs to be done with the Real-Time PCR machine and analysis software to make the output agree with the visible gel results. Once the Real-Time results can be confirmed by gel analysis, the threshold values given for each stress sample can be compared, and conclusions drawn about *pcm2* expression following stress. Microarray data in similar experiments leads us to anticipate that *pcm2* transcription will increase during heat shock, but not during osmotic shock.

The failure of Pcm2p to affect phenotypes may be due to the presence of another *S. pombe* protein whose function can compensate for loss of Pcm2p. Loss of PIMT function causes

problems in many other organisms; there is no reason to suggest that PIMT is simply unimportant in *S. pombe*. A synthetic lethal screen is a powerful method to identify such genes. I have now completed several initial screenings and have isolated five potential mutants.

Many steps of the synthetic lethal screen have been completed so far; however, there are still several additional steps that need to be done. The potential synthetic lethal mutants must be further screened to ensure that the mutation causing the inability to sector is actually in a gene whose product can compensate for loss of *pcm2*. In some cases, a mutation in a gene whose product influences membrane permeability could cause inability to sector, or a mutation in a gene whose product is part of the adenine pathway could make the cell appear red even if it has lost the plasmid. There are a number of other mutations that could give a false positive result during the initial screen. The next two steps of the synthetic lethal screen, the plasmid shuffle and the backcrossing, ensure that we will be left only will strains with legitimate synthetic lethal mutations.

In the plasmid shuffle, each of the potential synthetic lethal mutants will be transformed with *pNMT:pcm2/Leu2*. Each doubly transformed strain must prove itself to be able to sector, by losing *pNPT/ADE1-3/pcm2*, on PM –leucine –adenine media. A double mutant that successfully does this would appear initially red and then become white as it lost *pNPT/ADE1-3/pcm2*. As described earlier, this ensures that *pNPT/ADE1-3/pcm2* has not integrated into the genomic DNA, and ensures that the yeast has been unable to sector because of its reliance on the *pNPT/ADE1-3/pcm2*'s functional *pcm2*.

Any mutants that successfully complete the plasmid shuffle will then take part in a series of backcrosses. Since the mutagenesis likely resulted in more than one mutation per cell, each original potential synthetic lethal strain (such as KBP4; not the double-transformed mutant) must

be backcrossed three times with LNP35t, each time selecting for cells that are unable to sector. This will give final strains that are identical to LNP35t except for the mutation in the compensating gene. Three backcrosses is enough to statistically ensure that any additional mutations, those not pertaining to Pcm2p function, will be crossed out.

These backcrossed strains can then be used to identify the compensating gene. Genetic complementation using an *S. pombe* cDNA library will be utilized. The final backcrossed strains will be transformed with plasmids containing various genes from the library. Like in the plasmid shuffle, if cells are able to sector (i.e. lose *pNPT/ADE1-3/pcm2*) once they acquire a second plasmid, this means that the second plasmid must contain either *pcm2* or a compensating gene. Thus, any cell that is able to sector with the presence of the new plasmid will be selected. The library plasmid from these cells can be isolated and its inserted gene will be identified by DNA sequencing.

The five potential mutants isolated in this project were obtained by screening $1.65 * 10^5$ colonies. I expect that several of these will be eliminated in subsequent steps. Although the number of synthetic interactors is low, this is not without precedent. A recent genome-wide screen for synthetic interactors in budding yeast revealed that this number could vary from 0 to 146 (Tong et al 2004). The isolation and identification of this gene from one of these five mutants would confirm the importance of PIMT in *S. pombe* by indicating the presence of a redundant mechanism to prevent loss of essential PIMT function.

References

Bennett, E.J., J. Bjerregaard, J.E. Knapp, D.A. Chavous, A.M. Friedman, W.E. Royer, and C.M. O'Connor. 2003. Catalytic implications from the Drosophila protein L-isoaspartyl methyltransferase structure and site-directed mutagenesis. *Biochemistry.* 42:12844-12853.

Brennan, T.V., J.W. Anderson, Z. Jia, E.B. Waygood, and S. Clarke. 1994. Repair of spontaneously deamidated Hpr phosphocarrier protein catalyzed by the L-isoaspartate-(D-aspartate) *O*-methyltransferase. *The Journal of Biological Chemistry*. 269:24586-24595.

Chavous, D.A., F.R. Jackson, and C.M. O'Connor. 2001. Extension of the *Drosophila* lifespan by overexpression of a protein repair methyltransferase. *Proceedings of the National Academy of Sciences of the United States of America.* 98:14814-14818.

Chen, D., W.M. Toone, J. Mata, R. Lyne, G. Burns, K. Kivinen, A. Brazma, N. Jones, and J. Bähler. 2003. Global Transcription Responses of Fission Yeast to Environmental Stress. *Molecular Biology of the Cell.* 14:214-229.

Forsburg, S.L. 1993. Comparison of *Schizosaccharomyces pombe* expression systems. *Nucleic Acids Research*. 21:2955-2956.

Geiger, T. and S. Clarke. 1987. Deamidation, isomerization, and racemization at asparaginyl and aspartyl residues in peptides. *The Journal of Biological Chemistry.* 262:785-794.

Griffith, S.C., M.R. Sawaya, D.R. Boutz, N. Thapar, J.E. Katz, S. Clarke, and T.O. Yeates. 2001. Crystal structure of a protein repair methyltransferase from *Pyrococcus furiosus* with its L-isoaspartyl peptide substrate. *Journal of Molecular Biology.* 313:1103-1116.

Johnson, B.A., E.D. Murray Jr., S. Clarke, D.B. Glass, and D.W. Aswad. 1987. Protein carboxyl methyltransferase facilitates conversion of atypical L-isoaspartyl peptides to normal l-aspartyl peptides. *The Journal of Biological Chemistry.* 262:5622-5629.

Johnson, B.A., S.Q. Ngo, and D.W. Aswad. 1991. Widespread phylogenetic distribution of a protein methyltransferase that modifies L-isoaspartyl residues. *Biochemistry International.* 24:841-847.

Kagan, R.M. and S. Clarke. 1994. Widespread occurrence of three sequence motifs in diverse S-adenosylmethionine-dependent methyltransferases suggests a common structure for these enzymes. *Archives of Biochemistry and Biophysics.* 310:417-427.

Kagan, R.M., A. Niewmierzycka, and S. Clarke. 1997. Targeted gene disruption of the *Caenorhabditis elegans* L-isoaspartyl protein repair methyltransferase impairs survival of dauer stage nematodes. *Archives of Biochemsitry and Biophysics.* 348:320-328.

Kim, E., J.D. Lowenson, D.C. MacLaren, S. Clarke, and S.G. Young. 1997. Deficiency of a protein-repair enzyme results in the accumulation of altered proteins, retardation of growth, and fatal seizures in mice. *Proceedings of the National Academy of Sciences of the United States of America.* 94:6132-6137.

Lowenson, J.D., E. Kim, S.G. Young, and S. Clarke. 2001. Limited accumulation of damaged proteins in L-isoaspartyl (D-aspartyl) O-methyltransferase-deficient mice. *The Journal of Biological Chemistry.* 276:20695-20702.

Martin, J.L. and F.M. McMillan. 2002. SAM (dependent) I AM: the S-adenosylmethionine-dependent methyltransferase fold. *Current Opinion in Structural Biology.* 12:783-793.

Mata, J., R. Lyne, G. Burns, and J. Bähler. 2002. The transcriptional program of meiosis and sporulation in fission yeast. *Nature Genetics.* 32;143-147.

McFadden, P.N. and S. Clarke. 1987. Conversion of isoaspartyl peptides to normal peptides: implications for the cellular repair of damaged proteins. *Proceedings of the National Academy of Sciences of the United States of America.* 84:2595-2599.

Ryttersgaard, C., S.C. Griffith, M.R. Sawaya, D.C. MacLaren, S. Clarke, and T.O. Yeates. 2002. Crystal structure of human L-isoaspartyl methyltransferase. *The Journal of Biological Chemistry*. 277:10642-10646.

Schmitt, M.E., T.A. Brown, and B.L. Trumpower. 1990. A rapid and simple method for preparation of RNA from *Saccharomyces cerevisiae*. *Nucleic Acids Research*. 18:3091-3092.

Skinner, M.M., J.M. Puvathingal, R.L. Walter, and A.M. Friedman. 2000. Crystal structure of protein isoaspartyl methyltransferase: a catalyst for protein repair. *Structure with Folding and Design.* 8:1189-1201.

Smith, C.D., M. Carson, A.M. Friedman, M.M. Skinner, L. Delucas, L. Chantalat, L. Weise, T. Shirasawa, and D. Chattopadhyay. 2002. Crystal structure of human L-isoaspartyl-O-methyl-transferase with S-adenosyl homocysteine at 1.6-Å resolution and modeling of an isoaspartyl containing peptide at the active site. *Protein Science*. 11:625-635.

Tong, A.H.Y., G. Lesage, G.D. Bader, H. Ding, H. Xu, X. Xin, J. Young, G.F. Berriz, R.L. Brost, M. Chang, Y. Chen, X. Cheng, G. Chua, H. Friesen, D.S. Goldberg, J. Haynes, C. Humphries, G. He, S. Hussein, L. Ke, N. Krogan, Z. Li, J.N. Levinson, H. Lu, P. Ménard, C. Munyana, A.B. Parsons, O. Ryan, R. Tonikian, T. Roberts, A.-M. Sdicu, J. Shapiro, B. Sheikh, B. Suter, S.L. Wong, L.V. Zhang, H. Zhu, C.G. Burd, S. Munro, C. Sander, J. Rine, J. Greenblatt, M. Peter, A. Bretscher, G. Bell, F.P. Roth, G.W. Brown, B. Andrews, H. Bussey, and C. Boone. 2004. Global Mapping of the Yeast Genetic Interaction Network. *Science*. 303:808-813.

Visick, J.E., H. Cai, and S. Clarke. 1998. The L-isoaspartyl protein repair methyltransferase enhances survival of aging *Escherichia coli* subjected to secondary environmental stresses. *Journal of Bacteriology*. 180:2623-2629.

Yamamoto, A., H. Takagi, D. Kitamura, H. Tatsuoka, H. Nakano, H. Kawano, H. Kuroyanagi, Y. Yahagi, S. Kobayashi, K. Koizumi, T. Sakai, K. Saito, T. Chiba, K. Kawamura, K. Suzuki, T. Watanabe, H. Mori, and T. Shirasawa. 1998. Deficiency in protein L-isoaspartyl methyltransferase results in a fatal progressive epilepsy. *The Journal of Neuroscience*. 18:2063-2074.

Acknowledgements

Most importantly, I would like to thank my advisor, Dr. Clare O'Connor, for giving me the wonderful opportunity to work in her lab for the last three years. She is really a gifted scientist and teacher; I am so grateful to have been able to work with and learn from her.

I'd also especially like to thank the rest of the O'Connor Lab. Luke Northern – thank you for teaching me how to work with yeast, and for all of your help as I took over your project. Dean Wagner and Linda Tanini – you have both been so generous with your time, always available to help me out. I really value both your friendship and your willingness to teach me. Chris Levasseur, Karie Heinecke, and Jim Casey – thank you for your help with this project. Krissy Pattin, Heather DeFoer, and Damien LaRock – thanks for your friendship over the past three years; we've had a good time! I'd also like to thank Dr. Janet Paluh, Dr. Charles Hoffman, and Dr. Mohammed Shahabuddin for their generosity in giving advice and allowing me to use their equipment.

Also, thank you to Noah Patel for seeing me through the last stages of this project, always ready to listen and provide countless pep-talks. Finally, I'd especially like to thank the fabulous ladies of D22, who put up with me during the stressful times and heard me say the words "I'm going to lab" as I ran out the door at odd hours of the evening many more times than they ever should have. Claire Walters (thanks for getting through this with me – we made it!), Christi Crowley, Val LaVoie, Sara Hart, and Kristyn Bunce – you have all become family to me over the last four years – I treasure our time here together. Thank you for your constant support and encouragement. I couldn't have done this without any of you.